The Analysis of Tumor Microenvironment of Prostate Cancer Identifies Prognostic Signatures

Guoliang Lu
Department of Urology, Ruijin Hospital North, School of medicine, Shanghai Jiaotong University, 999 Xiwang Road, Shanghai 201801, China

Xiaojing Wang
Department of Urology, Ruijin Hospital North, School of medicine, Shanghai Jiaotong University, 999 Xiwang Road, Shanghai 201801, China

Baoxing Huang
Department of Urology, Ruijin Hospital North, School of medicine, Shanghai Jiaotong University, 999 Xiwang Road, Shanghai 201801, China

Yang Zhao
Department of Urology, Ruijin Hospital North, School of medicine, Shanghai Jiaotong University, 999 Xiwang Road, Shanghai 201801, China

Yuan Shao
Department of Urology, Ruijin Hospital North, School of medicine, Shanghai Jiaotong University, 999 Xiwang Road, Shanghai 201801, China

Dawei Wang (wdwrjhn@163.com)
Shanghai Jiao Tong University Medical School Affiliated Ruijin Hospital

---

Research

Keywords: Tumor microenvironment, TMEscore, prognostic signatures, Prostate cancer

Posted Date: October 16th, 2020

DOI: https://doi.org/10.21203/rs.3.rs-92274/v1

Abstract

Background: Tumor microenvironment (TME) is an essential part of tumor tissue, and increasing references suggested that TME has clinicopathological significance in predicting prognosis and therapeutic efficacy. However, little efficacy has been demonstrated in prostate cancer.

Methods: The cohort TCGA-PRAD (n=477) was used in this study. Based on the proportion of 22 types of immune cells calculated by CIBERSORT, TME was classified by K-means Clustering and differentially expressed genes (DEGs) were determined. Then TMEscore was calculated based on cluster signature genes, which were obtained from DEGs by random forest method, and the samples were classified to two subtypes. We performed somatic mutation and copy number variation analysis to identify the genetic characteristics of the two subtypes. Correlation analysis was performed to explore the correlation between TMEscore and the tumor response to ICIs as well as the prognosis of PCa.

Results: Based on the proportion of immune cells, we constructed the TMEscore model and classified PCa samples into TMEscore high and TMEscore low groups. The results of survival analysis suggested that the TMEscore high group had significantly better survival outcome than the TMEscore low group. The correlation analysis showed a significantly positive correlation between TMEscore and the known prognostic factors of tumors.

Conclusion: our study indicates that the TMEscore may be a potential prognostic biomarker in PCa. A comprehensive description of the characteristics of TME may help to explain the response to therapies for PCa patients and provide the new strategies for treatment.

Background

Prostate cancer (PCa) remains the most frequently diagnosed non-cutaneous malignancy among men, and the second most common cause of cancer death worldwide [1, 2]. Prognosis and treatment decisions of PCa are based on the malignant grade using the Gleason sum, the clinical stage using the tumor, node, metastasis system, and a patient's serum PSA level [3, 4]. Despite these well-used clinical predictive and prognostic factors, drastically variable outcomes are observed between PCa patients with similar stages and malignant grades [5]. Therefore, it has highlighted the importance of identifying novel biomarkers for the PCa prognostic assessment.

The tumor microenvironment (TME) is the cellular environment where the tumor located, mainly consisting of immune cells, mesenchymal cells, endothelial cells, inflammatory mediators, and extracellular matrix (ECM) molecules [6]. In the TME, the immune and stromal cells are the two major types of non-tumor components [7]. It is reported that the activated immune cells in the TME can promote tumor growth and progression[8]. Besides, the increasing references suggest that the TME cells have clinicopathological significance in predicting prognosis and therapeutic efficacy of tumors [4, 5]. In various malignancies, including gastric cancer and glioma, the gene signatures from the TME significantly associated with outcomes of patients [6, 9]. Although the landscape of TME has been widely

focused across a range of tumor types, little efficacy was demonstrated in PCa. Researchers found the TME in PCa is complex and dynamic[8]. Recent studies revealed a significant role of the TME cells in the initiation and progression of PCa [10, 11]. Importantly, a series of cell intrinsic changes in combination with distinct changes in the TME involve in the initiating events in PCa. The experimental data has uncovered the relationship between the TME cells and malignant tumor cells in which early changes in normal tissue microenvironment can promote tumorigenesis and in turn tumor cells can promote further pro-tumor changes in the microenvironment [2]. Moreover, it's worth noting that the abundance of immune cells and other cells in the TME can be estimated using computational methods [12, 13]. Several studies using these methodologies have explored the clinical utility of TME infiltrates [9, 14], and several mechanisms associated with the role of TME in immunotherapy response and resistance have been experimentally identified for some tumor types. However, the comprehensive profile of the TME infiltrating cells and TME characterization has not yet been elucidated in PCa.

In the present study, we estimated the TME infiltration patterns of PCa patients and constructed the TMEscore to predict their prognosis. We systematically analyzed the TMEscore-related phenotypes with genomic and clinical features of PCa. As a result, we identified a list of microenvironment-related signatures from the high/low TMEscore subtype that can predict survival outcomes pretty well in PCa. Our results demonstrate that the TMEscore could be a robust prognostic biomarker and predictive factor for the developing new diagnosis strategies in PCa.

Methods

Prostate cancer data collection

The transcriptional sequencing data of PCa patients (TCGA-PRAD) were separately downloaded from the TCGA database (https://xenabrowser.net/datapages) and the Gene Expression Omnibus (GEO) database (https://www.ncbi.nlm.nih.gov/geo/). The clinical information including gender, age, and survival time was also downloaded from TCGA and GEO. After removing the PCa samples without survival data or clinical data, 477 transcriptome samples from TCGA were selected as test sets, and 111 samples from GEO were used as validation sets (Table 1). The SNP data of these 477 samples were obtained from the TCGA database. Among the 477 samples, the SNP6 copy number segments of 471 samples were available from http://firebrowse.org/.

Table 1
Basic information of PCa patients

Series accession numbers	Platform used	No. of input patients	AJCC_Stage	Mean age[min, max]	Region	Survival outcome
TCGA-PRAD	Illumina RNAseq	477	NA	61.6[42, 79]	NA	DFS
GSE70770	Illumina HumanHT-12 V4.0 expression beadchip	111	NA	60.5[41, 73]	UK	RFS

TME analysis

The proportion of immune cells was calculated using the CIBERSORT algorithm with the leukocyte gene signature matrix (LM22) as the reference and with 1000 permutations [12]. TME clusters were determined using the ConcensusClusterPlus R package based on the proportion of immune cells [15]. The optimum clusters number K was estimated by algorithms elbow and gap statics. The limma R package was used to analyze the differentially expressed genes (DEGs) among the TME clusters, with thresholds of $p < 0.05$ and $|logFC| > 0.58$. Cluster signature genes were obtained by random forest method, and functional enrichment analysis was performed using ClusterProfiler R package. Cluster signature genes were classified to two categories according to cox coefficient (positive or negative) based on cox regression model[16]. TMEscore was calculated as follows:

$$TMEscore = \sum log_2(X+1) - \sum log_2(Y+1)$$

X represents the expression value of cluster signature genes with a positive cox coefficient, and Y represents the expression value of cluster signature genes with a negative cox coefficient.

The *maxstat* R package was used to define the optimal breakpoint for TMEscore, thus the 477 PCa samples were classified to high TMEScore and low TMEScore group. The TMEsore model was validated in Cohort GSE70770 from GEO.

Mutation spectrum analysis

We analyzed the mutational spectrum and mutational signatures of 477 samples from TCGA-PRAD by maftools and SomaticSignatures R packages. Copy number variable regions (CNVRs), including chromosomal CNV regions and minimal common regions (MCRs), were detected by GISTIC. Based on the results of CNVs, tumor purity and ploidy were estimated by ABSOLUTE R package.

Correlation analysis

We used Kaplan-Meier method to illustrate the relationship between the survival of PCa samples and the genetic signatures, such as miRNA, mRNA and the methylation site. We also explored the correlation between TMEscore and tumor response to ICIs in PCa. The tumor response to ICIs was evaluated by Tumor Immune Dysfunction and Exclusion (TIDE) scoring system, in which the higher the TIDE score, the worse the tumor response to ICIs and the worse the prognosis. Statistical significance was defined as two-tailed *P* values < 0.05.

Results

TME cell infiltrating patterns and DEGs associated with TME

We calculated the proportion of immune cells in 477 PCa samples, according to the previous findings that immune cells, especially tumor infiltering lymphocytes, are more related to the prognosis and immunotherapy effect of patients than the stromal cells in the TME[6, 17]. We depicted a comprehensive profile of the immune cell interactions, lineages and their effects on the OS of PCa patients, and obtained four distinct patterns of TME cell infiltration (Fig. 1A). The cell cluster A was characterized by the infiltration of the macrophages (M0), B cells (naïve), mast cells (resting) and so on. The cell cluster B was characterized by the infiltration of mast cells (activated), neutrophils, NK cells (activated) and so on. The cell cluster C and cluster D was characterized by the infiltration of the $CD4^+$ T cells (memory resting) and the macrophages (M2), respectively. According to the proportion of immune cells, the PCa samples can be divided into three TME clusters through consensus clustering analysis (Figure S1A-C). Interestingly, by mapping the TME clusters to the proportion of immune cells, we found significant differences in the distribution of immune cells among different TMEcluster samples, and TMEcluster 1 and 2 were quite different from TMEcluster 3 (Fig. 1B). The survival analysis showed that the survival was not significantly different among the three TME clusters (Fig. 1C). Unexpectedly, the TME clusters directly classified by the proportion of immune cells cannot distinguish the prognosis of PCa. It is probably due to the redundant information caused by LM22 gene. In order to reduce redundant information interference, we used an unsupervised clustering method to re-cluster 477 PCa samples based on the expression profile of TME-infiltrating phenotype related differential genes, and a total of 3637 DEGs were obtained. After dimensionality reduction by random forest algorism, the most relevant signature genes (n = 104) were used to classify the 477 samples into two clusters (Fig. 1D). These genes are mainly enriched in the pathways involved in immune activation, such as neutrophil chemotaxis, positive regulation of alpha-beta T cell activation, regulation of alpha-beta T cell differentiation, neutrophil migration and so on (Fig. 1E).

Construction of the TMEscore model for PCa samples

Based on the re-clustering model, we evaluated the correlation between DEGs and prognosis. The Cox regression model was used to evaluate the relationship between the DEGs and OS of PCa samples.

According to the coefficient value of genes, the 477 samples were classified into two groups with the TMEscore high (n = 308) and TMEscore low (n = 169) phenotype (x=-0.31).

As shown in Fig. 2A, the prognosis of the TMEscore high group was significantly better than that of the TMEscore low group. A comprehensive comparison of different TME clusters (Fig. 2B) showed that cluster samples based on immune cell components and proportions were notably correlated with the DEGs and TMEscore. Consistent with these findings, the TMEscore of the 111 PCa samples from the GEO can also reflect the prognosis of samples (Fig. 2C and 2D).

Correlation of the mutational signatures with the TMEScore phenotypes in PCa

The common genomic mutations, such as SNPs, have been reported to be used as predictors of aggressive prostate cancer. The exploration of characteristic SNPs would enable more accurate risk stratification, allowing for tailored management of individual prostate cancer [18]. Therefore, we further explored the relationship between the genomic mutations and TMEScore. The somatic mutation analysis showed that the most common mutation in PCa is the missense mutation, mainly caused by SNP, and C > T is the most common type of SNP mutations (Figure S2).The frequently mutated genes in TMEscore high group and TMEscore low group were presented in Fig. 3A and 3B, respectively, and their variant allele fractions (VAFs) were different between two groups (Fig. 3C). The contribution of 96 base substitution types was presented in Figure S3A and B. The mutational signature analysis showed that TMEscore high group was mainly related to signature1, signature3 and signature5 (Fig. 3E), and TMEscore low group was mainly related to signature1, signature5 and signature6 (Fig. 3F). It can be seen that there are significant differences in mutation characteristics between TMEscore high group and TMEscore low group.

MSI is an emerging biomarker used to predict the outcome of cancer treatment, and patients with MSI-H usually have better prognosis than those with MSI-L/MSS. The correlation analysis between TMEScore and MSI showed that the high TMEscore was significantly associated with MSI-H (Fig. 3D), and was associated with a good prognosis.

Correlation of copy number variants with the TMEScore phenotypes in PCa

We analyzed the correlation between the TMEscore and the characteristic of the chromosome CNV in PCa. The results showed that there were significant differences in chromosome copy number amplifications or deletions between the two TMEscore related phenotypes. The CNVs analysis by GISTIC showed that amplifications of chromosomal arms 8p, 8q, 7p and 7q, and deletions of chromosomal arms 8p, 18p, 18q and 16q frequently occurred in TMEscore-high subtype (Fig. 4A, C); amplifications of chromosomal arms 8p, 8q, 7p and 7q, and deletions of chromosomal arms 8p and 18q frequently occurred in TMEscore-low subtype (Fig. 4B, D). There were significant differences in MCRs between TMEscore high group and TMEscore low group. In the TMEscore high group, 14 amplifications and 30 deletions were detected, in which 3q26.2 amplification and 8p21.3 deletion were most significant (Fig. 4E); while in the TMEscore low group, 22 amplifications and 24 deletions were detected, in which

8q24.21, 8q21.13 amplifications and 6q14.3, 13q14.13 deletions were most significant (Fig. 4F). We also analyzed the correlation of tumor purity and tumor ploidy with the TMEScore related phenotypes, and the results showed no significant correlations (Figure S3C, D).

Comprehensive analysis of genomic signatures associated with the TMEscore in PCa

Based on the TMEscore phenotypes, we conducted a comprehensive analysis of the genomic signatures associated with the prognosis of PCa. DEG analysis obtained 5 differentially expressed miRNAs and 127 differentially expressed mRNAs between TMEscore-high and TMEscore-low subtypes, with the threshold $P < 0.05$ and $|logFC|>1$ for miRNA, and $|logFC|>1$ and $P < 0.05$ for mRNA, respectively. Among them, has-mir-133b (Fig. 5A) and *FMOD* (Fig. 5B) were most significantly correlated with survival of PCa. As DNA methylation status is closely related to tumor progression and prognosis, we performed differential methylation analysis between the TMEscore high and TMEscore low groups, and 38 significantly differential methylation sites were obtained, among which cg03804126 was most significantly correlated with OS (Fig. 5C). Moreover, a comprehensive genomic landscape of PCa was presented in Fig. 5D. We found 12 survival-related genes, including *CD38, PROK1, SRD5A2, TMEM35, DPT,FAM107A, SPOCK3, MT1G, SLC22A3, ANO7, MYLK* and *PTN*.

Discussion

In recent years, TME signatures representing TME status have been identified, and their potential clinical relevance in several cancers has been evaluated [9, 18, 19]. In the present study, we focused on the TME signatures that contribute to survival of PCa samples from the TCGA database and the GEO database. Based on the TME infiltration pattern analysis of 477 PCa patients, our observations suggested that the infiltrating immune cells such as macrophages (M2), $CD4^+$ T cells (memory resting), T cells (regulatory), Plasma cells and T cells (follicular) were closely related to the survival outcome of PCa patients. Interestingly, the results of our bioinformatic findings are consistent with some of the experimental studies. For example, in prostate cancer, most (but not all) pathological studies found that the greater the number of tumor-associated macrophages, the worse the prognosis [20, 21]. Additionally, the M2 macrophages were reported to be associated with higher stage and higher Gleason scores of tumors [22]. Researchers also found that regulatory T cells were elevated in the circulation of patients with PCa, and the elevated number of regulatory T cells was associated with worse prognosis [23].

Most importantly, we constructed the TMEscore model that is related to prognosis of PCa. Consistent with the results of previous studies on other types of tumors[6, 9], PCa patients with the TMEscore high phenotype have obviously better prognosis. Furthermore, the efficacy of TMEscore on prognosis was compared with other common prognostic factors. As described in the previous report, the common genetic variants SNP may act as predictors of aggressive prostate cancer, and would enable more accurate risk stratification in PCa [24]. Meanwhile, it is reported that MSI did not correlate with clinical stage, but might play a role in the development of a subset of prostate cancers. The MSI-H/dMMR molecular phenotype is uncommon in prostate cancer, but it has therapeutic significance [25]. Here, we

found a strong positive correlation between TMEscore and SNP or MSI-H in PCa. The results indicated that the TMEscore may be useful in developing new diagnostic strategies for PCa.

In order to explore other potential prognostic signatures, we integrated the genomic, clinical and pathological features of PCa samples. Expectantly, we obtained a list of prognostic signatures, including miRNAs, mRNA and methylation sites. As well known, miRNAs are short, endogenous RNAs in cells, promoting translational repression and/or destabilizing target mRNAs to optimize protein levels in numerous biologic processes [26]. The miRNA expression profiles of PCa have been reported [27], and miRNAs can act as oncomiRs or tumor suppressors in a multitude of cancers [28]. Numerous studies have been published, showing that the alterations in miRNAs are associated with initiation and progression of PCa [27]. Moreover, a list of miRNAs, such as miR-133b and miR-1, are novel biomarkers with prognostic and diagnostic value for recurrence of PCa and have been identified by miRNA expression profiling [29]. Consistent with these findings, we identified miR-133b with the most significant prognostic value from the TMEscore model in the PCa. In addition, *FMOD* has been reported as a potential biomarker for PCa [30]. We also identified the *FMOD* with the most significant prognostic value from the mRNA profile between TMEscore high/low groups. These results highlight the important role of TMEscore in recognizing prognostic signatures. Although the TMEscore phenotype of PCa can provide an alternative set of biomarkers with good prognostic ability, these results alone are not sufficient for clinical application. Hence, further validation, especially genetic and experimental studies involving larger samples, should be needed in the future.

Conclusions

In conclusion, the comprehensive assessment of the cellular, molecular and genetic factors associated with TMEscore in PCa patients, has provided several important insights into how prostate tumors respond to survival outcomes and may guide the development of new diagnostic strategies.

Abbreviations

TME: Tumor microenvironment; PCa: Prostate cancer; DEGs: Differentially expressed genes; ECM: extracellular matrix; CNVRs: Copy number variable regions; MCRs: minimal common regions; TIDE: Tumor Immune Dysfunction and Exclusion; VAFs: variant allele fractions; MSI: microsatellite instability; GO: Gene Ontology; DFS: Disease-free survival

Declarations

Ethics approval and consent to participate

Not applicable.

Consent for publication

Not applicable

Availability of data and materials

The datasets used and/or analyzed during the current study are available from the corresponding author on reasonable request.

Competing interests

The authors declare that they have no conflict of interest.

Funding

Not applicable

Authors' contributions

Conceptualization, Guoliang Lu; Data curation, Xiaojing Wang and Dawei Wang; Formal analysis, Dawei Wang; Investigation, Guoliang Lu and Baoxing Huang; Methodology, Guoliang Lu and Yang Zhao; Project administration, Dawei Wang; Resources, Dawei Wang; Software, Yuan Shao and Guoliang Lu; Supervision, Guoliang Lu and Dawei Wang; Visualization, Xiaojing Wang; Writing – original draft, Guoliang Lu; Writing – review & editing, Guoliang Lu and Dawei Wang.

Acknowledgements

We thank Shanghai Tongshu Biotechnology Co., Ltd. for support of bioinformatics technology.

References

1. Shukla, M. E., Yu, C., Reddy, C. A., Stephans, K. L., Klein, E. A., Abdel-Wahab, M., Ciezki, J. & Tendulkar, R. D. (2015) Evaluation of the current prostate cancer staging system based on cancer-specific mortality in the surveillance, epidemiology, and end results database, *Clinical genitourinary cancer.* **13**, 17-21.
2. Shiao, S. L., Chu, G. C. & Chung, L. W. (2016) Regulation of prostate cancer progression by the tumor microenvironment, *Cancer letters.* **380**, 340-8.
3. Crawford, E. D., Ventii, K. & Shore, N. D. (2014) New biomarkers in prostate cancer, *Oncology.* **28**, 135-42.
4. Bray, F., Lortet-Tieulent, J., Ferlay, J., Forman, D. & Auvinen, A. (2010) Prostate cancer incidence and mortality trends in 37 European countries: an overview, *European journal of cancer.* **46**, 3040-52.
5. McAllister, M. J., Underwood, M. A., Leung, H. Y. & Edwards, J. (2019) A review on the interactions between the tumor microenvironment and androgen receptor signaling in prostate cancer, *Translational research : the journal of laboratory and clinical medicine.* **206**, 91-106.

6. Jia, D., Li, S., Li, D., Xue, H., Yang, D. & Liu, Y. (2018) Mining TCGA database for genes of prognostic value in glioblastoma microenvironment, *Aging.* **10**, 592-605.
7. Sun, D. Y., Wu, J. Q., He, Z. H., He, M. F. & Sun, H. B. (2019) Cancer-associated fibroblast regulate proliferation and migration of prostate cancer cells through TGF-beta signaling pathway, *Life sciences.* **235**, 116791.
8. Kim, J. & Bae, J. S. (2016) Tumor-Associated Macrophages and Neutrophils in Tumor Microenvironment, *Mediators of inflammation.* **2016**, 6058147.
9. Zeng, D., Li, M., Zhou, R., Zhang, J., Sun, H., Shi, M., Bin, J., Liao, Y., Rao, J. & Liao, W. (2019) Tumor Microenvironment Characterization in Gastric Cancer Identifies Prognostic and Immunotherapeutically Relevant Gene Signatures, *Cancer immunology research.* **7**, 737-750.
10. Taverna, G., Pedretti, E., Di Caro, G., Borroni, E. M., Marchesi, F. & Grizzi, F. (2015) Inflammation and prostate cancer: friends or foe?, *Inflammation research : official journal of the European Histamine Research Society [et al].* **64**, 275-86.
11. De Marzo, A. M., Platz, E. A., Sutcliffe, S., Xu, J., Gronberg, H., Drake, C. G., Nakai, Y., Isaacs, W. B. & Nelson, W. G. (2007) Inflammation in prostate carcinogenesis, *Nat Rev Cancer.* **7**, 256-69.
12. Newman, A. M., Liu, C. L., Green, M. R., Gentles, A. J., Feng, W., Xu, Y., Hoang, C. D., Diehn, M. & Alizadeh, A. A. (2015) Robust enumeration of cell subsets from tissue expression profiles, *Nature methods.* **12**, 453-7.
13. Becht, E., Giraldo, N. A., Lacroix, L., Buttard, B., Elarouci, N., Petitprez, F., Selves, J., Laurent-Puig, P., Sautes-Fridman, C., Fridman, W. H. & de Reynies, A. (2016) Estimating the population abundance of tissue-infiltrating immune and stromal cell populations using gene expression, *Genome biology.* **17**, 218.
14. Fu, H., Zhu, Y., Wang, Y., Liu, Z., Zhang, J., Xie, H., Fu, Q., Dai, B., Ye, D. & Xu, J. (2018) Identification and Validation of Stromal Immunotype Predict Survival and Benefit from Adjuvant Chemotherapy in Patients with Muscle-Invasive Bladder Cancer, *Clinical cancer research : an official journal of the American Association for Cancer Research.* **24**, 3069-3078.
15. Sorlie, T., Perou, C. M., Tibshirani, R., Aas, T., Geisler, S., Johnsen, H., Hastie, T., Eisen, M. B., van de Rijn, M., Jeffrey, S. S., Thorsen, T., Quist, H., Matese, J. C., Brown, P. O., Botstein, D., Lonning, P. E. & Borresen-Dale, A. L. (2001) Gene expression patterns of breast carcinomas distinguish tumor subclasses with clinical implications, *Proceedings of the National Academy of Sciences of the United States of America.* **98**, 10869-74.
16. Ritchie, M. E., Phipson, B., Wu, D., Hu, Y., Law, C. W., Shi, W. & Smyth, G. K. (2015) limma powers differential expression analyses for RNA-sequencing and microarray studies, *Nucleic acids research.* **43**, e47.
17. Lang, J. M. (2019) Understanding dynamic interactions in the prostate tumor microenvironment, *Urologic oncology.* **37**, 532-534.
18. Wolff, C., Zoschke, C., Kalangi, S. K., Reddanna, P. & Schafer-Korting, M. (2019) Tumor microenvironment determines drug efficacy in vitro - apoptotic and anti-inflammatory effects of 15-

lipoxygenase metabolite, 13-HpOTrE, *European journal of pharmaceutics and biopharmaceutics : official journal of Arbeitsgemeinschaft fur Pharmazeutische Verfahrenstechnik eV.* **142**, 1-7.

19. Pfannstiel, C., Strissel, P. L., Chiappinelli, K. B., Sikic, D., Wach, S., Wirtz, R. M., Wullweber, A., Taubert, H., Breyer, J., Otto, W., Worst, T., Burger, M., Wullich, B., Bolenz, C., Fuhrich, N., Geppert, C. I., Weyerer, V., Stoehr, R., Bertz, S., Keck, B., Erlmeier, F., Erben, P., Hartmann, A., Strick, R., Eckstein, M., Bridge Consortium, G., Bridge Consortium, G., Bridge Consortium, G. & Bridge Consortium, G. (2019) The Tumor Immune Microenvironment Drives a Prognostic Relevance That Correlates with Bladder Cancer Subtypes, *Cancer immunology research.* **7**, 923-938.
20. Shimura, S., Yang, G., Ebara, S., Wheeler, T. M., Frolov, A. & Thompson, T. C. (2000) Reduced infiltration of tumor-associated macrophages in human prostate cancer: association with cancer progression, *Cancer Res.* **60**, 5857-61.
21. Nonomura, N., Takayama, H., Nakayama, M., Nakai, Y., Kawashima, A., Mukai, M., Nagahara, A., Aozasa, K. & Tsujimura, A. (2011) Infiltration of tumour-associated macrophages in prostate biopsy specimens is predictive of disease progression after hormonal therapy for prostate cancer, *BJU international.* **107**, 1918-22.
22. Lanciotti, M., Masieri, L., Raspollini, M. R., Minervini, A., Mari, A., Comito, G., Giannoni, E., Carini, M., Chiarugi, P. & Serni, S. (2014) The role of M1 and M2 macrophages in prostate cancer in relation to extracapsular tumor extension and biochemical recurrence after radical prostatectomy, *BioMed research international.* **2014**, 486798.
23. Ebelt, K., Babaryka, G., Frankenberger, B., Stief, C. G., Eisenmenger, W., Kirchner, T., Schendel, D. J. & Noessner, E. (2009) Prostate cancer lesions are surrounded by FOXP3+, PD-1+ and B7-H1+ lymphocyte clusters, *European journal of cancer.* **45**, 1664-72.
24. Benafif, S., Kote-Jarai, Z., Eeles, R. A. & Consortium, P. (2018) A Review of Prostate Cancer Genome-Wide Association Studies (GWAS), *Cancer epidemiology, biomarkers & prevention : a publication of the American Association for Cancer Research, cosponsored by the American Society of Preventive Oncology.* **27**, 845-857.
25. Antonarakis, E. S., Shaukat, F., Isaacsson Velho, P., Kaur, H., Shenderov, E., Pardoll, D. M. & Lotan, T. L. (2019) Clinical Features and Therapeutic Outcomes in Men with Advanced Prostate Cancer and DNA Mismatch Repair Gene Mutations, *European urology.* **75**, 378-382.
26. Valencia-Sanchez, M. A., Liu, J., Hannon, G. J. & Parker, R. (2006) Control of translation and mRNA degradation by miRNAs and siRNAs, *Genes & development.* **20**, 515-24.
27. Pashaei, E., Pashaei, E., Ahmady, M., Ozen, M. & Aydin, N. (2017) Meta-analysis of miRNA expression profiles for prostate cancer recurrence following radical prostatectomy, *PloS one.* **12**, e0179543.
28. Shenouda, S. K. & Alahari, S. K. (2009) MicroRNA function in cancer: oncogene or a tumor suppressor?, *Cancer metastasis reviews.* **28**, 369-78.
29. Karatas, O. F., Guzel, E., Suer, I., Ekici, I. D., Caskurlu, T., Creighton, C. J., Ittmann, M. & Ozen, M. (2014) miR-1 and miR-133b are differentially expressed in patients with recurrent prostate cancer, *PloS one.* **9**, e98675.

30. Bettin, A., Reyes, I. & Reyes, N. (2016) Gene expression profiling of prostate cancer-associated genes identifies fibromodulin as potential novel biomarker for prostate cancer, *The International journal of biological markers.* **31**, e153-62.

Figures

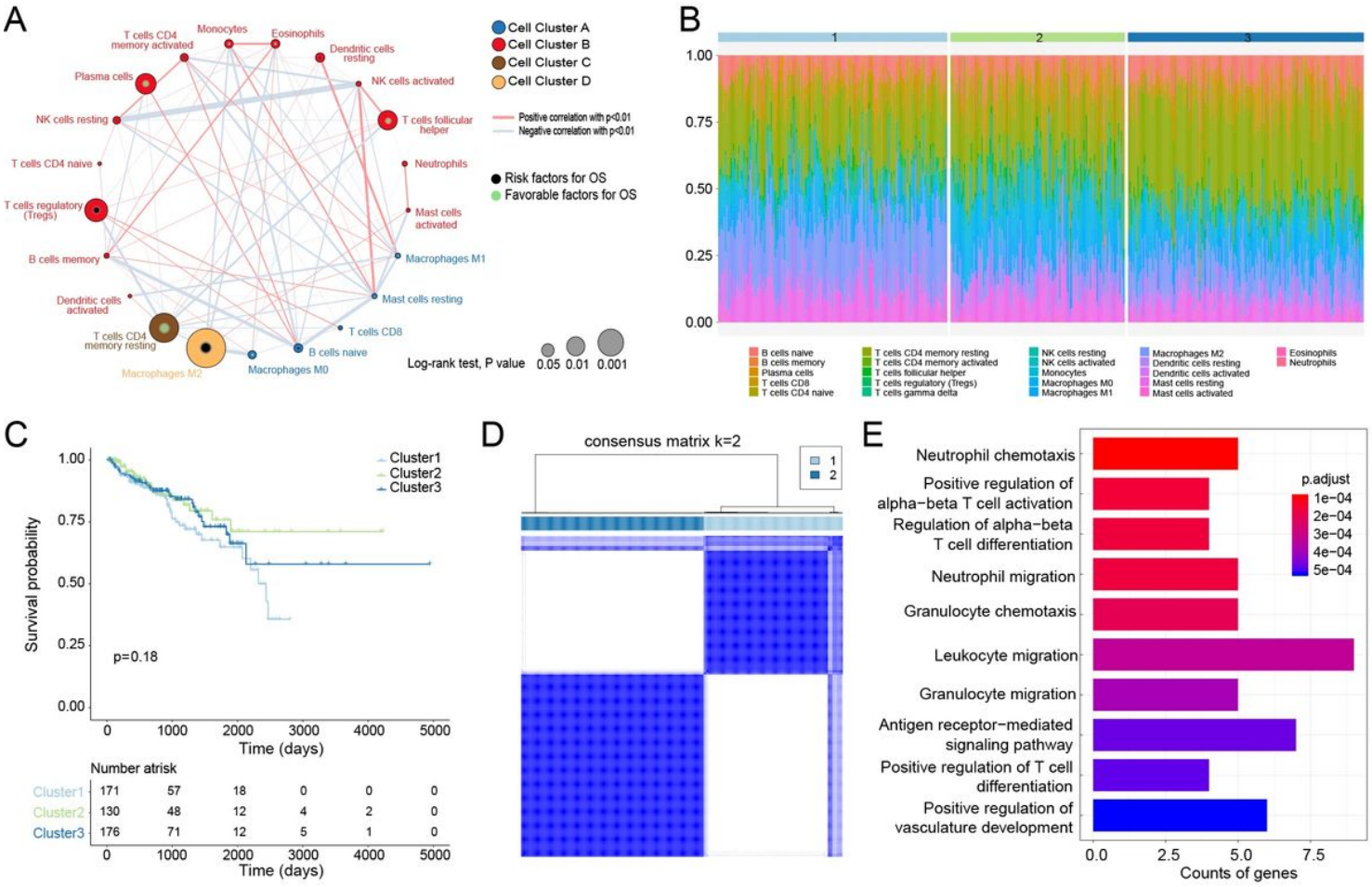

Figure 1

The TME cell infiltrating patterns and characteristic of the TME cluster. (A) The cellular interaction of TME infiltrating cell types. Cell cluster A, blue; Cell cluster B, red; Cell cluster C, brown; Cell cluster D, yellow. The size of each cell represents survival impact of each TME cell type. The risk for overall survival is indicated in black, and the favor for overall survival is indicated in green. The lines connecting TME infiltrating cells represent cellular interactions. The thickness of the line represents the strength of correlation. Positive correlation is indicated in red and negative correlation in blue. (B) The proportion of the TME infiltrating cells and the Unsupervised clustering of them for 477 CaP patients. TMEcluster 1, light blue; TMEcluster 2, green; TMEcluster 3, dark blue. (C) Kaplan-Meier curves for survival of 477 CaP samples with the three TMEclusters. The number of patients in TMEcluster 1, 2 and 3 phenotypes are 171, 130, and 176, respectively. Log-rank test showed P = 0.18. (D) The consensus matrix of 477 samples for k=2, displaying the clustering stability using 1000 iterations of hierarchical clustering. (E) The Gene Ontology (GO)

enrichment analysis of the TMEscore-related DEGs. The x axis indicates the number of genes within each GO term.

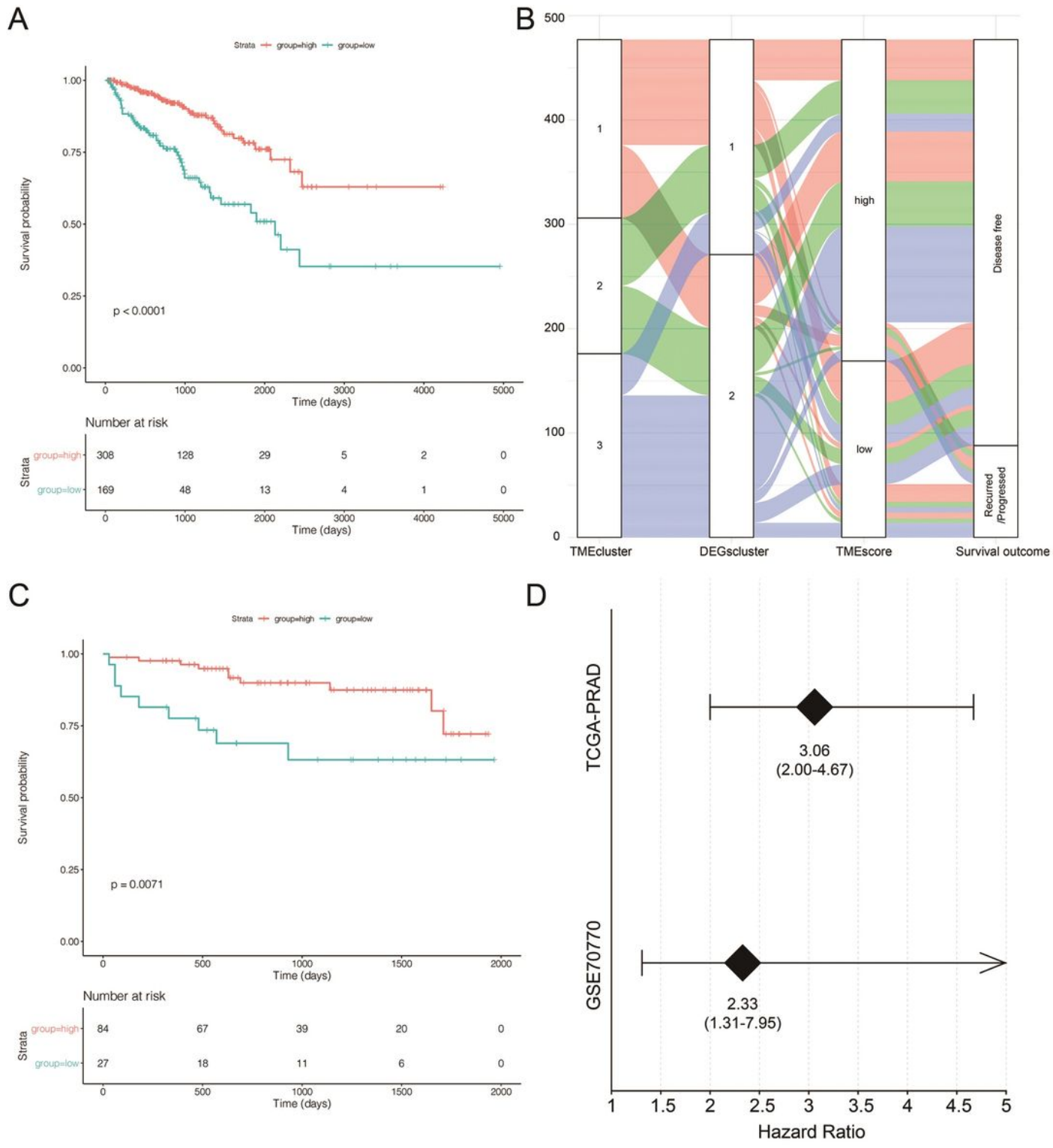

Figure 2

The prognostic characteristics of the TMEsore related phenotypes in CaP. (A) Kaplan-Meier curves for TMEscore high and TMEscore low patients from TCGA database. (Log-rank test, P < 0.0001). (B) Alluvial diagram of TME gene-clusters in groups with different DEGs cluster, TMEscore, and survival outcomes.

(C) Kaplan-Meier curves for TMEscore high and TMEscore low patients from GEO database. (Log-rank test, P < 0.01). (D) The forest plot for survival analysis of different data sets.

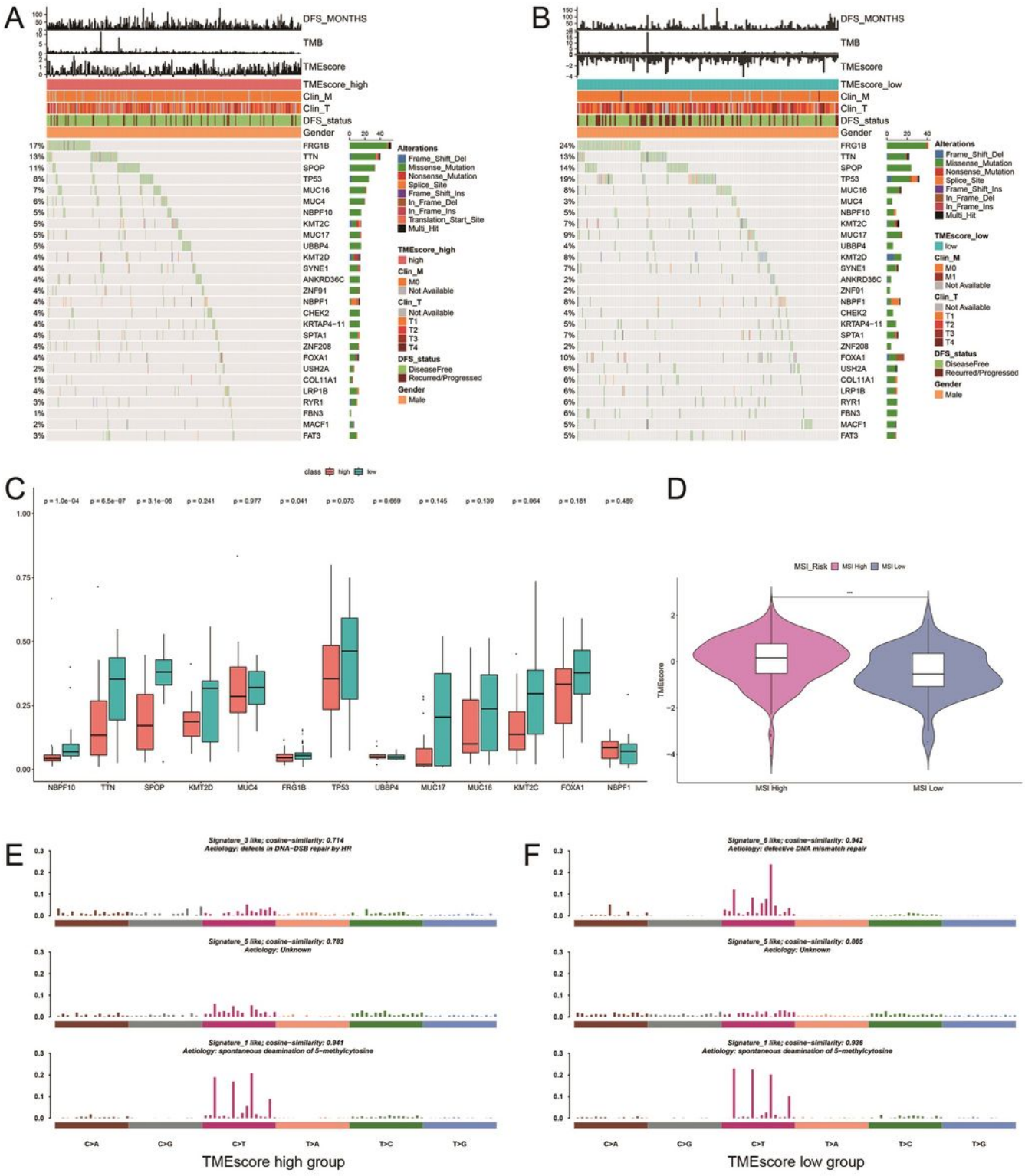

Figure 3

The somatic genome characteristics of the TMEsore related phenotypes in CaP. The distribution of frequently mutated genes in TMEscore high group (A) and TMEscore low group (B) in CaP. Different colors indicate different alterations. The upper barplot indicates TMB, TMEscore, and Disease-free

survival (DFS) per patient, whereas the left barplot shows the mutation frequency of each gene in separate TMEscore groups. The patient annotations show the TMEscores, TCGA molecular subtypes, TMEscore, gender, and survival status. (C) The variant allele fractions of frequently mutated genes in TMEscore high and TMEscore low groups. Within each group, the scattered dots represent mean value of signature genes. The thick line represents the median value. (D) Violin plot showing the TMEscores in groups with different microsatellite instability (MSI) status. The Kruskal-Wallis test were used to compare the differences between two groups. Mutational signatures associated with TMEscore high group (E) and TMEscore low group (F).

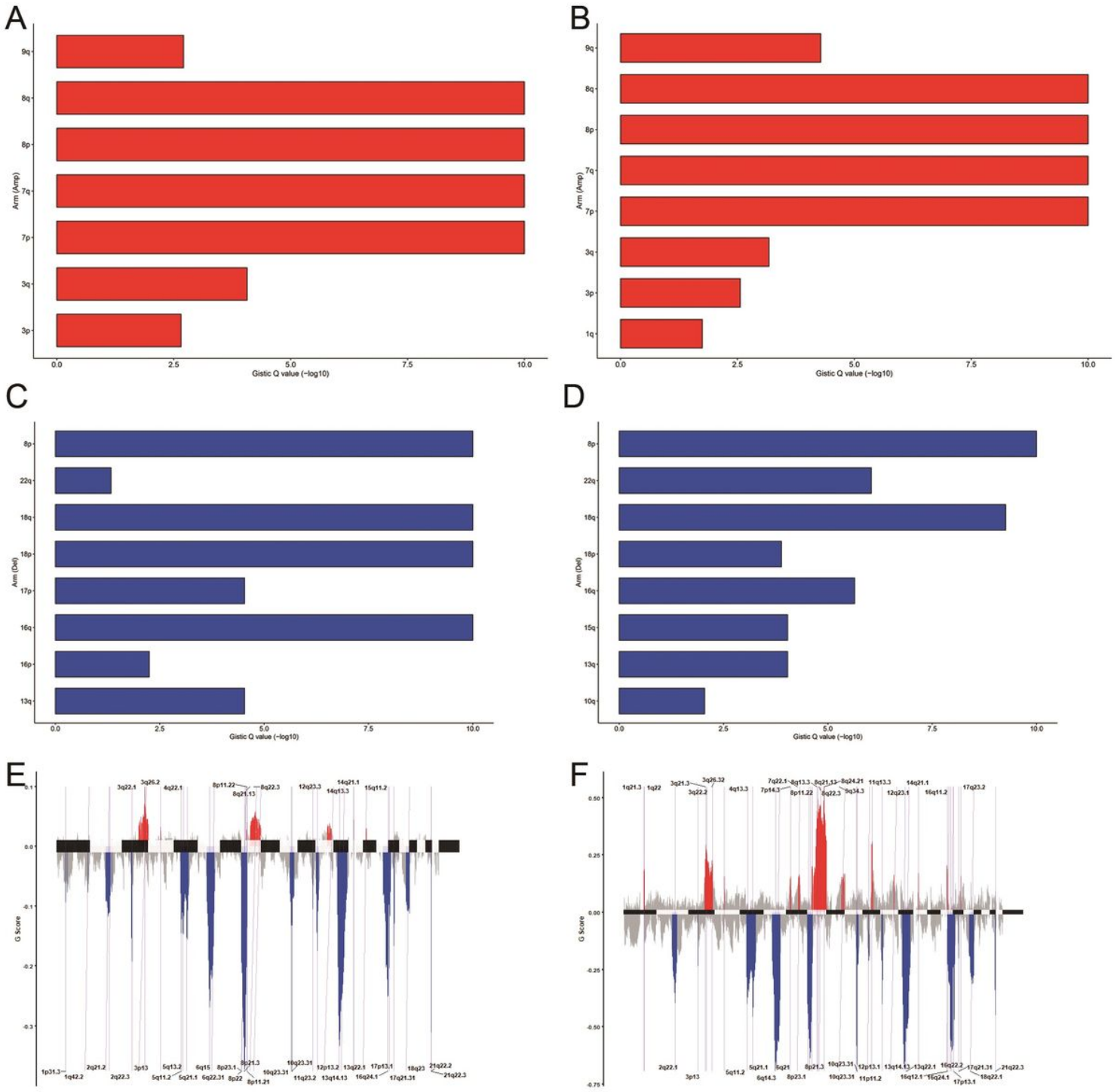

Figure 4

The copy number variant characteristics of the TMEscore related phenotypes in CaP. The amplification regions of chromosome arm in the TMEscore high group (A) and TMEscore low group (B). The deletion regions of chromosome arm in the TMEscore high group (C) and TMEscore low group (D). The transverse axis indicates the Gistic Q value of the chromosome arm. The minimal common regions (MCRs) of copy number variations in the TMEscore high group (E) and TMEscore low group (F).

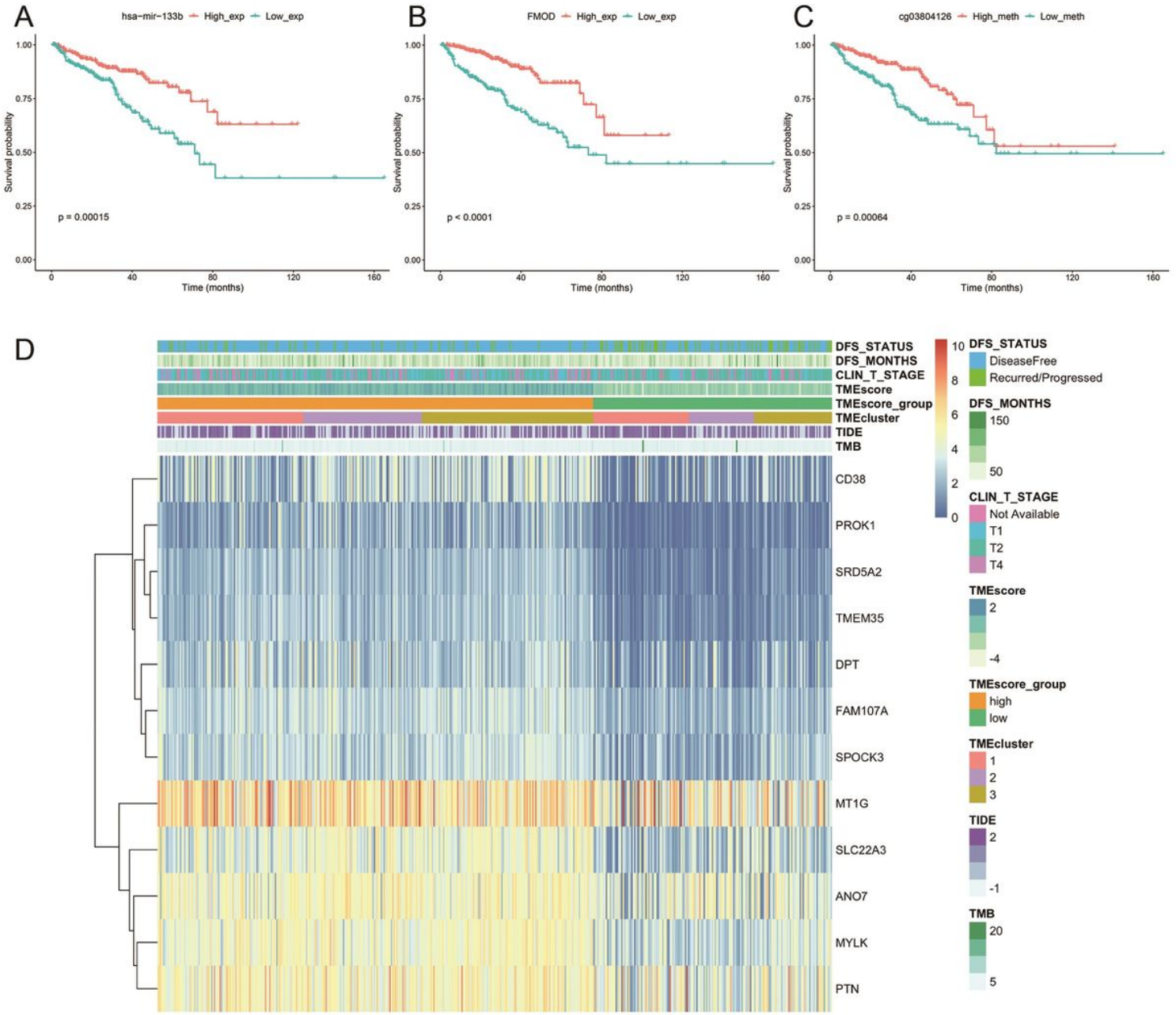

Figure 5

The prognostic genomic signatures associated with the TMEsore related phenotypes in CaP. (A) The Kaplan-Meier survival curve was generated for the selected differential miRNA from the comparison of TMEscore high and TMEscore low groups. (B) The Kaplan-Meier survival curve was generated for the

selected differential mRNA from the comparison of TMEscore high and TMEscore low groups. (C) The Kaplan-Meier survival curve was generated for the selected differential methylation sites from the comparison of TMEscore high and TMEscore low groups. (D) The heat map of the prognostic DEGs based on expression data derived from the TMEscore high/low groups.

Supplementary Files

This is a list of supplementary files associated with this preprint. Click to download.

- Supplementarymaterials.docx